

AN ARTIFICIAL NEURAL NETWORK MODELING OF SOLAR ASSISTED HEAT PUMP SYSTEM FOR BUILDINGS

Ceyhun Yılmaz^{1*}, İsmail Koyuncu², Önder Kaşka³

¹Mechanical Engineering Department, Afyon Kocatepe University, Afyonkarahisar, Turkey

²Electrical and Electronics Engineering Department, Afyon Kocatepe University, Afyonkarahisar, Turkey

³Mechanical Engineering Department, Osmaniye Korkut Ata University, Osmaniye, Turkey

Corresponding author: Ceyhun Yılmaz, e-mail: ceyhunyilmaz@aku.edu.tr

REFERENCE NO	ABSTRACT
ACON-02	In this study, the solar assisted heat pump system is modeled in the Matlab program using the MLFF-ANN structure. In the Matlab-based MLFF-ANN structure, 10 neurons containing 6 TanSig TF neurons in the hidden layer and Pureline TF in the output layer are used. The training performance of the design is calculated to be 5.13×10^{-9} and the test performance is calculated to be 9.4×10^{-4} . The system components were of a solar collector (flat plate), a heat pump, and a storage tank founded to heat a controlled room in yard of Mechanical Engineering Department, University of Gaziantep, Turkey. The data were taken between March 1 and March 29. The coefficient of performance of the heat pump (COPHP) was calculated about 2.2 for cloudy day and 3.65 for sunny day. Average exergy destruction of evaporator, condenser, compressor and expansion valves are 0.1445 kW, 0.1033 kW, 0.32 kW, 0.041 kW respectively.

Keywords:
Solar assisted heat pump,
Thermodynamic analysis, ANN,
FPGA.

1. INTRODUCTION

Solar energy systems are an attractive solution to reduce the use of non-renewable energy resources. In addition, space heating and water heating costs are also eliminated by this method. Those systems can be used for low temperature heating system and a solution for pollution, noise, high energy cost and fossil fuel consumption. Solar energy is mostly used during summer months (About 6 months) and during winter season (12 hour mismatch) for energy requirement of the buildings. Solar energy are mostly applied in Turkey and flat plate solar collectors widely used for heating at residential, air conditioning and industrial system [1].

Worldwide energy utilize continues to raise in spite of restrictions in fossil fuel energy sources. Moreover, global warming is effect due to the utilization of energy produced by fossil fuels and it is portended to lead to considerable climate alteration and great influence to society. Therefore many countries have attempted to reduce their energy utilize. The decreasing of global warming influence and reducing total energy utilize are effective by energy conservation, and also it assists extent the life of non-renewable energy sources [2]. In the recent decennium, heat pump systems (including

ground source heat pump and air source heat pump) have received huge attentiveness due to energy request rising and fossil fuels exhausting at an alarming average.

Solar energy and heat pump systems are good alternative energy for decreasing non-renewable energy resources, and also consuming cost of heating & cooling of space and water heating. The system can be used for low temperature heating system and a solution for pollution, noise, high cost receipt and fossil fuel consumption such as CO₂, SO_x, HC etc. Solar energy is mostly used during summer months (About 6 months) and during winter season (12 hour mismatch) for energy requirement of the buildings. Solar energy are mostly applied in Turkey and flat plate solar collectors widely used for heating at residential, air conditioning and industrial system. One of the solutions is energy storage (store heat of the solar energy for high loads) which used for seasonal and diurnal discrepancy. The type of energy storage (seasonal (long term) storage and daily (short term) storage) with most potential is the thermal energy storage because the fraction of heat in the national energy balances in Turkey is considerable. Energy storage is integrated into heat pump for satisfying heat demand and decreasing cost of energy source.

Ozgener and Hepbasli [3] studied on energy and exergy analysis of solar-assisted ground source heat pump greenhouse heating system (SAGSHPGHS) at Solar Energy Institute of Ege University, Izmir, Turkey. Some of the important outcomes which were obtained throughout the test duration 16th of December 2003 until 31st of March 2004. The COP prices for the heat pump different from 2.00 to 3.125, whilst the COP of the entire system were nearly 5-20% less than COP of the heat pump. The exergy efficiency prices for the entire system and the GSHP unit on a product/fuel basis were found to be 67.7 and 71.8%, respectively. Finally, this study will be very beneficial to the researcher transacting with heat pumps specially SAGSHP system. Suleman el at. [4] studied on energy and exergy analysis of an integrated solar heat pump system which was improved for industrial heating. The outcomes display that the energetic coefficient of performance (COP) of the heat pump cycle was 3.54 while the exergy efficiency was 42.5%. Furthermore, the energetic COP of the system was 2.97 and exergy efficiency of the system was 35.7%. The exergy efficiency of the process was 75% whilst the energy efficiency was 58%.

In this study, the modeled and test values are measured of the solar assisted heat pump system has been synthesized and tested for the Virtex-6 FPGA chip using the Xilinx ISE Design Tools System 14.1. Results of the performance analysis and FPGA chip statistics are investigated. Finally, sensitivity analysis is performed by comparing the actual experimental analysis results with the Matlab based and FPGA-based ANN constructions results of the system.

2. DESCRIPTION OF SOLAR ASSISTED HEAT PUMP SYSTEM

The schematic of solar assisted heat pump system is shown in Fig. 1. For this purpose, operational conditions are expressed as follow: The solar assisted heat pump heating system was designed and working conditions explained in detail as shown in Figure 1. Heat

pump is circulated as a water to water type and assumption as follow:

- Isentropic efficiency of compressor is 80 %, works under adiabatic state.
- Evaporator and condenser circulated flowing fluid (R-22) at constant pressure.
- There is no pressure loss in system.
- The R-22 of evaporator and condenser exist are saturated vapor or liquid states.

Before starting into energy and exergy analyses, all processes are assumed as steady-state and steady-flow with negligible potential and kinetic energy effects in an adiabatic form [5].

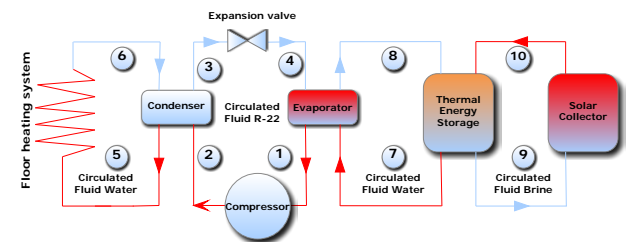


Figure 1. The solar assisted heat pump heating system (Modified from [6])

3. EXERGY RELATIONS FOR SYSTEM COMPONENTS

Irreversibility or the exergy destruction of the each individual component (i.e. compressor, and solar collectors) is computed by applying exergy balance over them so that their acts on the total exergy destruction of the SAHP can be expressed. The exergy balance relation for any steady state systems is

$$\dot{E}x_{in} - \dot{E}x_{out} - \dot{E}x_{loss} = 0 \quad (1)$$

Since exergy, like energy, can be transferred to or from a system in three forms: heat, work, and mass flow, first two terms of the equation (1) includes them if they exist. By undertaking the equation (2) exergy balance for insulated condenser is

$$(\dot{E}x_2 + \dot{E}x_5) - (\dot{E}x_3 + \dot{E}x_6) - \dot{E}x_{dest} = 0 \quad (2)$$

where $\dot{E}x_2$ and $\dot{E}x_3$ entering and leaving exergies to/from the condenser due to mass flow of the R22, and $\dot{E}x_5$, $\dot{E}x_6$ entering and leaving exergies to/from the condenser due to mass flow of the water, respectively. Equation (3) can be written in detail as

$$\begin{aligned} \dot{m}_{wc} [(h_5 - h_6) - T_o (s_5 - s_6)] + \\ \dot{m}_r [(h_2 - h_3) - T_o (s_2 - s_3)] - \dot{E}x_{dest} = 0 \end{aligned} \quad (3)$$

here, \dot{m}_{wc} and \dot{m}_r are mass flow rate of the water and mass flow rate of the refrigerant flowing through condenser, respectively. Mass flow rate of the water through the condenser are measured and the mass flow rate of the refrigerant is found by applying first law of the thermodynamic.

Exergy balance for evaporator is

$$(\dot{E}x_4 + \dot{E}x_7) - (\dot{E}x_1 + \dot{E}x_8) - \dot{E}x_{dest} = 0 \quad (4)$$

The two terms at the right hand side of the equation (4) denote the exergy that enter the evaporator and leave the evaporator, respectively, due to mass flow of R22 and water. And this equation is extracted as,

$$\begin{aligned} \dot{m}_{we} [(h_7 - h_8) - T_o (s_7 - s_8)] \\ + \dot{m}_r [(h_2 - h_3) - T_o (s_2 - s_3)] \\ - \dot{E}x_{dest} = 0 \end{aligned} \quad (5)$$

here, \dot{m}_{we} and \dot{m}_r are mass flow rate of the water and mass flow rate of the refrigerant flowing through evaporator, respectively. Mass flow rate of the water through the evaporator was measured.

Exergy balance for the compressor is,

$$\begin{aligned} (\dot{E}x_1 + \dot{W}_{comp}) - \left(\dot{E}x_2 + \left(1 - \frac{T_o}{T_b} \right) \dot{Q}_{Loss} \right) \\ - \dot{E}x_{dest} = 0 \end{aligned} \quad (6)$$

and the clear form of equation (6) is

$$\begin{aligned} \dot{m}_r [(h_1 - h_2) - T_o (s_2 - s_1)] + \dot{W}_{comp} \\ - \left(1 - \frac{T_o}{T_b} \right) \dot{Q}_{Loss} - \dot{E}x_{dest} = 0 \end{aligned} \quad (7)$$

\dot{Q}_{Loss} is the heat loss from the compressor and it is computed from the energy balance or the first law of the thermodynamic. First law relation for the compressor is

$$\dot{E}_{in} - \dot{E}_{out} = 0 \quad (8)$$

$$\dot{m}_r (h_2 - h_1) + \dot{W}_{comp} - \dot{Q}_{Loss} = 0 \quad (9)$$

and the exergy balance for the expansion valve is

$$\dot{E}x_3 - \dot{E}x_4 - \dot{E}x_{loss} = 0 \quad (10)$$

and clear form is

$$\dot{m}_r [(h_3 - h_4) - T_o (s_3 - s_4)] - \dot{E}x_{dest} = 0 \quad (11)$$

Inner energy storage having larger volume is used as heat sink for the evaporator. And the energy gained from the solar collector is stored in it.

4. EXERGY ANALYSIS RESULTS

System given in figure 1 was run during the heating period of February 14 through April 30, 2002. Results are used to determine exergy and the second law analysis of the SAHP. An Illustrative example will have given for March 1, 2012 and March 29, 2012. Detailed energy and first law analysis were given in [6].

An illustrative example is given in Table 1. Exergy analysis of the system is done by applying model given previously. Table 1 includes measured data of pressure, temperature and mass flow rate of the water loops in the system. While temperatures and pressures of refrigerant loop are measured, mass flow rate of the refrigerant given in the table was calculated from energy balance for the evaporator and the condenser. Corresponding specific enthalpy, specific entropy, specific energy, specific exergy, energy rate, exergy rate are also included in the table. State entropy values of the water-antifreeze solution were calculated by using constant specific heat values for %20 ethylene-glycol in water.

Table 1. Thermodynamic properties used in SAHP system.

State number	Item	Fluid	Mass flow rate \dot{m} (kg/s)	Temperature °C	Pressure p (kPa)	Specific enthalpy h (kJ/kg)	Specific entropy s (kJ/kg K)	Specific Exergy ψ (kJ/kg)	Energy rate $E=\dot{m}h$ (kW)	Exergy rate $E=\dot{m}\psi$ (kW)
0 (Dead state)		R22		19	101.3	425.3	1.969			
0 (Dead state)		Water		19	101.3	79.75	0,2819			
1	Compressor inlet	R22	0.0097	27.4	531	424.4	1.813	44.69	4.101	0.4319
2	Compressor outlet	R22	0.0097	92.4	1544	462.4	1.835	76.29	4.469	0.7372
3	Exp. Valve outlet	R22	0.0097	40.25	1544	251.3	1.172	58.82	2.428	0.5684
4	Exp. Valve inlet	R22	0.0097	1.98	531	251.3	1.186	54.55	2.428	0.5271
5	Condenser inlet	Water	0.0097	21	150	88.0	0.3104	-0.07046	2.405	-0.001925
6	Condenser outlet	Water	0.027	38.9	150	162.7	0.5569	2.605	4.446	0.07117
7	Evaporator inlet	Water	0.036	28.12	150	117.8	0.2533	0.4857	4.241	0.01749
8	Evaporator outlet	Water	0.036	17.01	150	71.3	0.4105	-0.07104	2.568	-0.002557

Figure 2-5 shows variation of exergy destructions and temperatures of heat pump systems run during March 1, 2001. Discontinuity in the graphs shows the hours at which heat pump does not work.

Figure 2 shows variation of exergy destruction and variations of T_1 , T_4 , T_7 , T_8 temperatures which are inlet and outlet temperatures of refrigerant and water respectively. Average exergy destruction occurred in evaporator is calculated 0.1445 kW. Averages values of the temperatures T_1 , T_4 , T_7 and T_8 are 33.3 °C, 3.7 °C, 33.9 °C and 22.5 °C respectively. Variation of inlet and outlet water temperature, inlet and outlet refrigerant temperature and exergy destruction occurred in the condenser is given in figure 6. Average exergy destruction in the condenser is 0.1033kW. Averages values of the temperatures T_2 , T_3 , T_5 and T_6 are 101.1°C, 40.8 °C, 21.45 °C and 41.57 °C respectively.

Average exergy destruction rate of the compressor and expansion valves are 0.32 kW and 0.041 kW respectively. Depend on the results; exergy destruction rate occurred in the heat pump components can be set in order from highest to lowest as compressor, evaporator, condenser and expansion valve. This result is convenient the result given in [7].

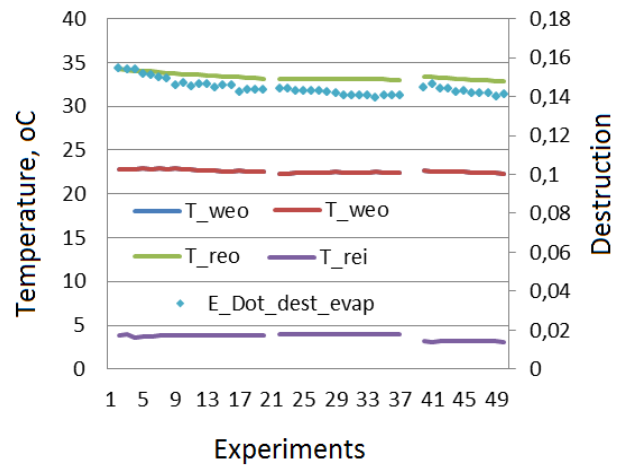


Fig 2. Exergy destructions and temperatures of evaporator.

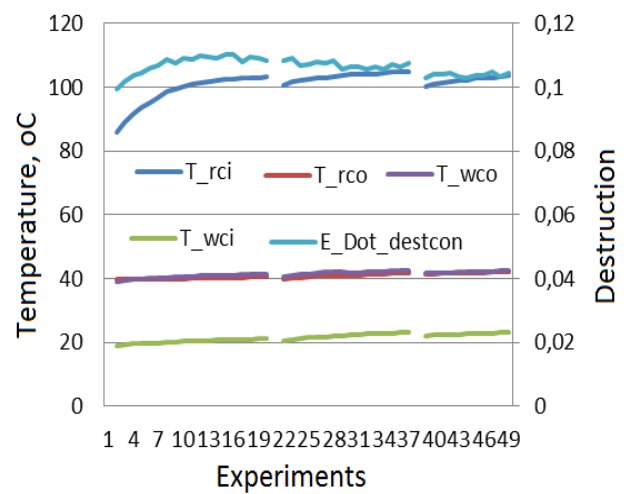


Fig 3. Exergy destructions and temperatures of condenser.

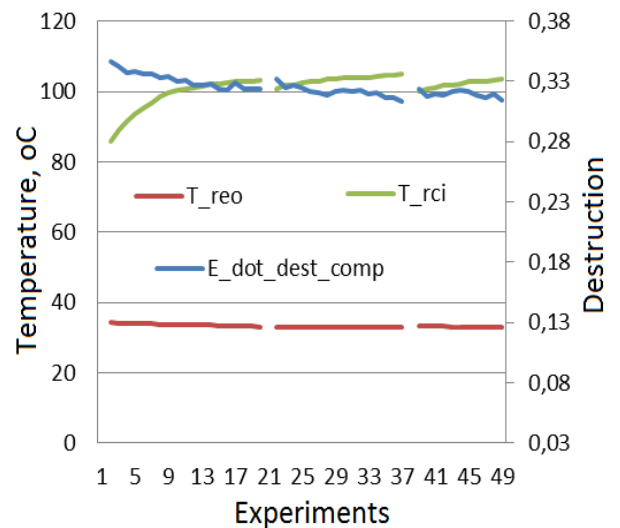


Fig 4. Exergy destructions and temperatures of compressor.

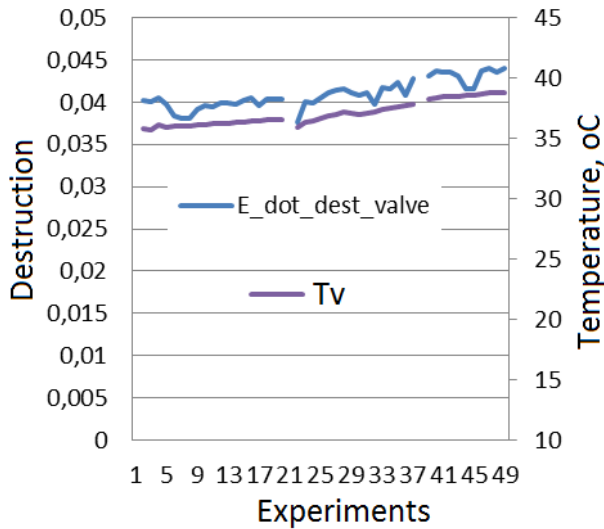


Fig 5. Exergy destructions and temperatures of expansion valve.

5. ANN-BASED SOLAR ASSISTED HEATING SYSTEM ON FPGA

Today's, Artificial Neural Networks (ANNs) are widely used in many research areas. These applications are included in the use of image processing [8], biomedical [9], modeling of oscillators [10], optimization [11], classification [12], and prediction [13]. ANNs can be implemented using different hardware structures, such as application specific integrated circuits (ASICs), digital signal processors (DSPs), and field programmable gate arrays (FPGAs). FPGA-based ANNs are preferred in the literature due to features such as repeatable programming [14] parallel signal processing [15] and high performance [16]. One of the number standards is used in FPGA chips is the 32-bit IEEE 754-1985 floating point number standard [17]. FPGA-based designs are coded using languages such as Verilog HDL [18] and VHDL (Very High Speed Integrated Circuit (VHSIC) Hardware Description Language) [19]. In this paper, the multi-layer feed forward (MLFF) ANN-based solar-assisted heat pump system is performed in the VHDL language on the FPGA using the 32-bit IEEE 754-1985 floating point number standard. The designed system is investigated and tested for the Virtex-6 FPGA chip using the Xilinx ISE Design Tools System 14.7 program. In the study, MLFF-ANN structure is firstly modeled in Matlab program. During

the modeling process, 640 data taken from the actual study results of the 10-input system with 10 inputs are divided into 480 training data and 160 data as test data. In the MLFF-ANN structure, there are 10 inputs and 10 outputs at the input layer. In the ANN hidden layer, 6 neurons containing TanSig TF and 10 neurons containing Pureline TF in the output layer are used. The Levenberg-Marquardt algorithm is used during the training phase and the ANN training performance is reached a mean squared error of 5.13×10^{-9} at the end of 365 epochs. And then, ANN is tested using 160 test data and ANN's test performance is calculated to be 9.4×10^{-4} . After the test process, the FPGA-based MLFF-ANN structure can be constructed with reference to the bias and weight values are used in the ANN and converted to a 32-bit floating point number. The MLFF-ANN-based solar-assisted heat pump system is coded in the VHDL language using the 32-bit IEEE 754-1985 floating-point number standard and processed for the Virtex-6 FPGA chip using the Xilinx ISE Design Tools System 14.7 program. Figure 6 shows the top level block diagram of the MLFF-ANN-based solar-assisted heat pump system which is designed on the FPGA.

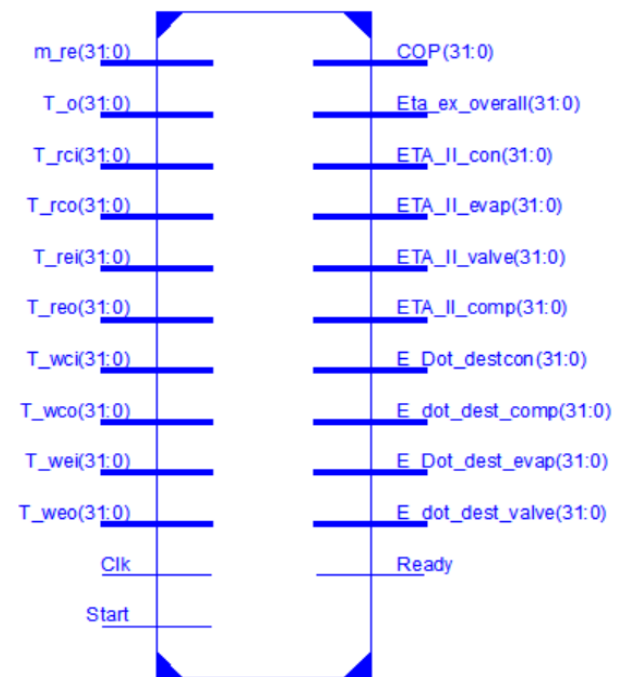


Fig. 6. The top level block diagram of ANN-based solar assisted heat pump system on FPGA.

$T_{reo}, T_{rci}, T_{rco}, T_{rei}, T_{wci}, T_{wco}, T_{wei}, T_{weo}, \dot{m}_{re}, T_0$ signals conforming to the 32-bit IEEE 754 - 1985 floating-point number standard at the inlet state of the FPGA-based system, and $E_{dot_dest_valve}, E_{dot_dest_comp}, ETA_II_comp, E_Dot_destcon, ETA_II_con, E_Dot_dest_evap, ETA_II_respond, COP$ and $Eta_ex_overall$ are the system output signals. The 1-bit Start signal is the control signal needed to start the system, and Clk is the system clock pulse signal. The designed FPGA-based system has a 1-bit Ready signal which is indicated that the output signals are generated and sent to the output. Figure 7 shows the second level block diagram of the MLFF-ANN-based solar-assisted heat pump system are designed on the FPGA.

The basic unit such as the multiplications and summations in the 32-bit floating point number standard are used in the MLFF-ANN-based solar assisted heat pump system is performed using the IP Core Generator developed by Xilinx ISE Design Tools. When

the $T_{reo}, T_{rci}, T_{rco}, T_{rei}, T_{wci}, T_{wco}, T_{wei}, T_{weo}, \dot{m}_{re}, T_0$ signals are sent to the ANN-based MLFF-ANN-based solar assisted heat pump system unit on the FPGA, these values are compared with weight values in the hidden layer is multiplied and the value obtained is summed with the bias value. Then, the *Tangent sigmoid* in the neuron is transferred through the transfer function and transferred to the neuron exit. The output values of neuron from here are connected in parallel to 10 neurons in the output layer. The obtaining values are multiplied by the weight values in the neurons in the output layer and summed with the bias value of each neuron. The obtained values are transferred through the purelin transfer function and transferred to the system output, and the ready signal value is to be unity (1). Up to the now, the filter unit has been designed so that output signals are not transmitted to the output. Since the FPGA-based design runs as a pipeline, the system generates 10 results in the every clock cycle.

3. CONCLUSIONS

An experimental system was found for calculating exergy analysis of a solar assisted heat pump space heating system during heating periods of March 1 and March 29 in Gaziantep, Turkey. The results were discussed. The exergy destruction of compressor, expansion valve, condenser and evaporator were plotted to compare with literature, also thermodynamic table of heat pump was given. All of the results have an agreement with literature work. Additionally, solar assisted heat pump system can be applied in Gaziantep and its' province. In this study, the solar assisted heat pump system is firstly modeled in the Matlab program using the MLFF-ANN structure. In the Matlab-based MLFF-ANN structure, 10 neurons containing 6 TanSig TF neurons in the hidden layer and Pureline TF in the output layer are used. The training performance of the design is calculated to be 5.13×10^{-9} and the test performance is calculated to be 9.4×10^{-4} . Using the Matlab-based ANN structure, the FPGA-based solar assisted heat pump system unit is conformed to the 32-bit IEEE 754-1985 floating point number standard that is coded in the VHDL language software. The designed system is processed for the Virtex-6 FPGA chip using the Xilinx ISE Design Tools System 14.7 program. In a future work, system performances can be investigated using different network structures and transfer functions.

Acknowledgements

This research has been supported by grant number 18.Kariyer.20 from Afyon Kocatepe University Scientific Research Projects Coordination Unit.

Nomenclature

T	Temperature (K)
h	Specific enthalpy (kJ/kg)
\dot{m}	Mass flow rate (kg/s)
\dot{Q}	Heat transfer rate (kW)
\dot{W}	Power (Kw)
\dot{E}	Exergy rate (kW)
ψ	Specific flow exergy (kJ/kg)

ε	Exergy efficiency
η	Energy efficiency

References

- [1] Kaska, O., Experimental Investigation of Performance of Solar Assisted Heat Pump Space Heating System With an Energy Storage, 2002, University of Gaziantep: Turkey.
- [2] Arunwattana, W., A model for improvement of water heating heat exchanger designs for residential heat pump water heaters 2010, Massey University: New Zealand.
- [3] Zhang, Y., Investigation on the application of heat pump systems in residential buildings in the UK, 2012, Coventry University: United Kingdom.
- [4] Salman, A., Experimental investigation on performance of a heating and cooling system with ground coupled heat pump, 2012, University of Gaziantep: Turkey.
- [5] Yumrutas, R., and Kaska, O., Experimental investigation of thermal performance of a solar assisted heat pump system with an energy storage. International Journal of Energy Research, 2004. **28**:163–175.
- [6] Dikici, A. and Akbulut A, Performance characteristics and energy–exergy analysis of solar-assisted heat pump system. Building and Environment 2008. **43**: 1961–1972
- [7] Çağlar, Ahmet, and Cemil Yamalı. "Performance analysis of a solar-assisted heat pump with an evacuated tubular collector for domestic heating." Energy and buildings 54 (2012): 22-28.
- [8] Paukštaitis, V., Dosinas, A.: Pulsed neural networks for image processing. Electronics and Electrical Eng. 95(7), 15–20 (2015).
- [9] Falahian, R., Dastjerdi, M.M., Molaie, M., Jafari, S., Gharibzadeh, S.: Artificial neural network-based modeling of brain response to flicker light. Nonlinear Dyn. 81(4), 1951–1967, 2015.
- [10] M. Alçın, İ. Pehlivan, İ. Koyuncu, Hardware design and implementation of a novel ANN-based chaotic generator in FPGA,

Elsevier, *Optik-International Journal for Light and Electron Optics*. Vol. 127(13), pp. 5500-5505, 2016.

[11] Betiku, E., Taiwo, A.E.: Modeling and optimization of bioethanol production from breadfruit starch hydrolyzate vis-à-vis response surface methodology and ANN. *Renewable Energy* 74, 87–94, 2015.

[12] Zang, W., Liu, X., Bi, W.: An artificial neural network classification model based on DNA computing. *Human Centered Computing Lecture Notes in Comp. Sci.* 8944, 880–889, 2015.

[13] Roy, S., Banerjee, R., Bose, P.K.: Performance and exhaust emissions prediction of a CRDI assisted single cylinder diesel engine coupled with EGR using artificial neural network. *Applied Energy* 119, 330–340, 2014.

[14] İ. Koyuncu, İ. Şahin, C. Gloster, N. K. Sarıtekin, A Neuron Library for Rapid Realization of Artificial Neural Networks on FPGA: A Case Study of Rössler Chaotic System, *Journal of Circuits, Systems and Computers*, Vol. 26(01), 1750015, 2017.

[15] Tuna M, Fidan CB. Electronic circuit design, implementation and FPGA-based realization of a new 3d chaotic system with single equilibrium point. *Optik-International Journal for Light and Electron Optics* 2016;127(24):11786–99.

[16] İ. Koyuncu, A. T. Özcerit, The design and realization of a new high speed FPGA-based chaotic true random number generator, Elsevier, *Computers & Electrical Engineering*, Vol. 58, pp. 203-214, 2017.

[17] E. Avaroğlu, İ. Koyuncu, A. B. Özer, M. Türk, Hybrid pseudo-random number generator for cryptographic systems, Springer, *Nonlinear Dynamics*, Vol. 82, pp. 239-248, 2015.

[18] İnceöz, E., Çavuş, E., FPGA Implementation of Variable-Length Split-Radix FFT Algorithm. *International Journal of Engineering Science*, Vol. 7, No: 7 pp. 13977-13980, 2017.

[19] Sahin, S., Cavuslu, M. A., FPGA Implementation of Wavelet Neural Network Training with PSO/iPSO. *Journal of Circuits, Systems and Computers*, 1850098., 2017.